International Journal of Bifurcation and Chaos, Vol. 30, No. 6 (2020) 2030014 (21 pages)

DOI: 10.1142/S0218127420300141

Bifurcation Sequences and Multistability in a Two-Dimensional Piecewise Linear Map

Wirot Tikjha*
Faculty of Science and Technology,
Pibulsongkram Rajabhat University,
Phitsanulok 65000, Thailand
Centre of Excellence in Mathematics,
PERDO, CHE, Thailand
wirottik@psru.ac.th

Laura Gardini
Department DESP, University of Urbino, Italy
laura.gardini@uniurb.it

Received March 3, 2019

Bifurcation mechanisms in piecewise linear or piecewise smooth maps are quite different with respect to those occurring in smooth maps, due to the role played by the borders. In this work, we describe bifurcation mechanisms associated with the appearance/disappearance of cycles, which may be related to several cases: (A) fold border collision bifurcations, (B) degenerate flip bifurcations, supercritical and subcritical, (C) degenerate transcritical bifurcations and (D) supercritical center bifurcations. Each of these is characterized by a particular dynamic behavior, and may be related to attracting or repelling cycles. We consider different bifurcation routes, showing the interplay between all these kinds of bifurcations, and their role in the phase plane in determining attracting sets and basins of attraction.

Keywords: Piecewise linear map; fold border collision bifurcation; flip border collision bifurcation; center bifurcation; subcritical or supercritical bifurcation.

1. Introduction

For more than two decades, the study of the dynamic behaviors and bifurcations occurring in piecewise smooth two-dimensional maps, has been considered in an increasing number of works, mainly due to their relevance in applications. In fact, both in the engineering context, as well as in biology, economics and social sciences, the final system to investigate is often not smooth. In engineering systems (electronics and mechanics) this mainly occurs because of switching manifolds, crossing which the system changes definition. Moreover, although these systems are often described in continuous time, the study of the bifurcations related to switching manifolds may be studied via Poincaré return maps on such manifolds, so that they are ultimately reduced to discrete time models, and piecewise smooth maps. Many examples can be found in [Banerjee & Verghese, 2001; Zhusubaliyev & Mosekilde, 2003; Brogliato, 1999; di Bernardo *et al.*, 2008; Ma *et al.*, 2006; Simpson, 2010]. In other disciplines, applied models are described directly in discrete time, and the introduction of switchings are quite common, representing changes in external policies or existing constraints. Examples of applications in economics and social sciences are in [Radi *et al.*, 2014; Radi & Gardini, 2015, 2018; Burr *et al.*, 2015; Bischi *et al.*, 2017; Gardini *et al.*, 2018].

*Author for correspondence

The common feature in many works is the characterization of what are nowadays called *border collision bifurcations*. This term was introduced for the first time in [Nusse & Yorke, 1992, 1995], and it is now widespread to represent the merging (or collision) of a periodic point with the set crossing which the map changes its definition. Such a crossing may lead to drastic changes in the invariant sets and the dynamics of the system. In particular, the collision may cause the disappearance of an attracting cycle and the appearance of any kind of dynamics: divergence, convergence to a cycle of different period, convergence to a chaotic attractor. The classification of the possible result of such a bifurcation is still mainly an open problem in the two-dimensional case. In fact, while for one-dimensional maps this classification (at least for codimension-one bifurcations) is quite complete, via the use of the skew-tent map, which represents the one-dimensional border collision normal form map (see [Sushko *et al.*, 2015] and references therein), for maps of the plane the theory is quite far from being complete. The two-dimensional border collision normal form map has been introduced in [Nusse & Yorke, 1992, 1995], it is a two-dimensional piecewise linear map in which the parameters are only trace and determinant of the linear functions in the two different partitions of the plane, separated by the border line $x = 0$, and this map has been investigated in many works. Dangerous bifurcations, leading to divergence at the bifurcation value, but to bounded dynamics before and after, which are particularly dangerous in electronic systems, have been considered in [Hassouneh *et al.*, 2004; Ganguli & Banerjee, 2005; Avrutin *et al.*, 2016]. One more dangerous occurrence in the applied context is multistability. In fact, when several coexisting attractors are present in the system, the related basins may be not simple, and may be intermingled in a chaotic way, so that a very small perturbation in the parameters of the systems may lead to a change of ω-limit set of the trajectories. In the two-dimensional border collision normal form map it has been shown that infinitely many attracting cycles can also coexist [Simpson, 2014a, 2014b]. Thus, it is quite important to find the regions in the parameter space where this occurs, often with the aim to avoid these cases.

Besides the border collision bifurcations, in piecewise linear maps (PWL for short henceforth) also the bifurcations which are standard in smooth systems, related to the eigenvalues of a cycle, behave in particular ways. While in the smooth linear case such bifurcations only occur for a fixed point leading to divergence, when a switching line exists, in piecewise linear maps, these bifurcations may occur to cycles of any period and the result is, in general, unpredictable. As remarked above, it can result in divergence, convergence to a cycle of different period, convergence to a chaotic attractor. Some studies related to the loss of stability via real or complex eigenvalues can be found in [Simpson & Meiss, 2008; Sushko & Gardini, 2008, 2010]. In particular, the transition via complex eigenvalues, called center bifurcation, has been characterized at the bifurcation value in [Sushko & Gardini, 2008], but without the analysis of the kind of bifurcation involved, that is, subcritical or supercritical, which cannot be studied by using only one map, since this result depends on the global properties of the piecewise definition, as investigated in one family of maps in [Gardini & Tikjha, 2019].

It is important to emphasize that in PWL maps, both the border collision bifurcations and the local bifucations of cycles (related to eigenvalues) may lead to the appearance/disappearance of cycles. However, these are not the only bifurcations, in fact, in this kind of systems a cycle may also appear/disappear via infinity. That is, a cycle of period $n \geq 1$ may have periodic points which approach infinity and then disappear (becomes virtual) or it may suddenly appear from infinity, with periodic points very far from the origin. This bifurcation is related to a zero value in the denominator of the analytic expressions of the periodic point of a cycle, and also to the transition of the characteristic polynomial of the Jacobian matrix of a suitable expression of T^n (related to the n-cycle) through the value $+1$. It is called degenerate transcritical bifurcation and described in [Sushko & Gardini, 2010]. Other properties related to the transition to infinity have been considered in [Avrutin *et al.*, 2010; Avrutin *et al.*, 2016].

In particular, we notice that the appearance/ disappearance of a cycle in a two-dimensional continuous PWL map may occur via a

(A) fold border collision bifurcation (fold-BCB for short), and (due to the continuity of the map) it is necessarily related to a pair of cycles, merging in a unique cycle at the bifurcation value;
(B) degenerate flip bifurcation (both of subcritical and supercrtical types), involving one unique

cycle after the bifurcation, and infinitely many at the bifurcation value;

(C) degenerate transcritical bifurcation, involving one unique cycle;

(D) supercritical center bifurcation, involving a pair of cycles after the bifurcation, and infinitely many at the bifurcation value.

Let us also recall here their roles and properties. We can consider a fixed point of map T, since in case of a cycle of period n we consider the map T^n for which the periodic points are fixed points, and the fixed point closest to LC_{-1} where the critical line LC_{-1} (following [Mira *et al.*, 1996]) is the set crossing which the map changes its definition.

(A) A fold-BCB occurs without any relation with the values of the eigenvalues. At the bifurcation value two cycles merge with a periodic point on the critical line LC_{-1}, and after the bifurcation two different cycles exist whose symbolic sequence differs for one symbol only. Thus, at the bifurcation value we can consider two different Jacobian matrices, one obtained by applying T_L to the critical point on LC_{-1} and the other obtained by applying T_R to that critical point. So the eigenvalues of these two different Jacobian matrices determine which kind of cycles exist after the bifurcation, whether saddle or attracting node or repelling node. Notice that in smooth maps only a saddle/attracting node or a saddle/repelling node can occur in a fold bifurcation, while here also two saddles may appear (we shall see examples).

(B) A degenerate flip bifurcation of a fixed point is related to one eigenvalue equal to -1 at the bifurcation value. As described in [Sushko & Gardini, 2010], assuming that the related eigenvector reaches the critical line LC_{-1} a segment is determined by this critical point, say c_{-1}, and its image c on the eigenvector, which is filled with cycles of period-2 (in general, if the map is T^n, of cycles of double period for T). Thus, the cycle with periodic points $\{c_{-1}, c\}$ is also a cycle at its border collision. If this cycle of double period does not exist when the fixed point is attracting, then after the bifurcation it will appear (so it can be considered a supercritical bifurcation), and the cycle of double period may appear attracting or repelling. Differently, when this cycle of double period (attracting or repelling) exists when the fixed point is attracting, then after the bifurcation it will disappear (so it can be considered a subcritical bifurcation). We shall see examples of both types.

(C) A degenerate transcritical bifurcation of a fixed point is related to one eigenvalue equal to $+1$ at the bifurcation value as well as to a vanishing denominator in the analytic expression of the periodic points. That is, crossing this value the sign of the periodic point changes, leading to the transition real/virtual or *vice versa* (see in [Sushko & Gardini, 2010]). Thus, a unique cycle is involved in this transition and when real it may be attracting or not (since there is no relation with the other eigenvalue, which may be inside the unit circle or outside).

(D) The center bifurcation studied in [Sushko & Gardini, 2008] describes the structure of the dynamics at the bifurcation value. At the bifurcation value (when the Jacobian determinant is 1) with complex eigenvalues the fixed point is a center, and we know that an invariant area exists, centered at the fixed point, with different properties depending on the rotation number, rational or irrational. When it is rational then the invariant area is a polygon bounded by a segment of critical line LC_{-1} and its images (whose number depends on the rotation), belonging to the closed partition which includes the considered fixed point, and the area is filled with periodic orbits of the same period, except for the fixed point. When the rotation is irrational the invariant area is bounded by an ellipse tangent to LC_{-1} which is the envelope curve of the images of a segment of LC_{-1} including the tangency point. This invariant area is filled with invariant ellipses with quasiperiodic orbits dense on the curves.

The exact dynamic behavior occurring at a center bifurcation value does not say which kind of bifurcation occurs, and which kind of dynamics will appear after (when the cycle becomes a repelling focus). So the bifurcation may be supercritical, leading to new attracting sets, or subcritical, or degenerate: the conservative case, area preserving.

When the center bifurcation occurs with a rational rotation number, in the supercritical case, it may lead (when the fixed point is a repelling focus) to the existence of a closed invariant attracting curve, which in general, consists of the connection of a pair of cycles, a saddle and an attracting node (unstable set of the saddle cycle), with the same rotation number at the bifurcation value. Roughly speaking, of the infinitely many cycles existing at the bifurcation, only two of them survive,

leading to a saddle-node connection, and the symbolic sequences of the two cycles differ for only one symbol, so that the attracting node has one periodic point on the opposite side of the fixed point, while the saddle cycle has two periodic points on that opposite side. Differently, the bifurcation may lead to an attracting closed invariant curve with quasiperiodic orbits dense on it.

In the subcritical case a repelling closed invariant curve exists when the fixed point is attracting. In general, the curve consists in the connection of a pair of cycles, a saddle and a repelling node (stable set of the saddle cycle), or in a repelling closed invariant curve with quasiperiodic orbits dense on it. This repelling curve binds the basin of attraction of the fixed point close to the bifurcation value, and it merges with the boundary of the invariant area at the subcritical bifurcation value.

Our goal in the present work is to show several occurrences of these different kinds of bifurcations, in the family of PWL maps considered in [Gardini & Tikjha, 2019] (which is a particular case of a family of maps proposed in [Tikjha *et al.*, 2017]), given by

$$T : \begin{cases} x' = |x| - ay, \\ y' = x - cy + d, \end{cases} \tag{1}$$

where a, c, and $d > 0$ are real parameters. The value of the parameter d is just a scaling factor, and we can consider $d = 1$ in the system given above. In that work, the bifurcation curves related to fixed points, 3-cycles and 4-cycles have been determined, and then only the center bifurcation of these cycles has been considered, determining its occurrence as supercritical or subcritical. Here we continue the investigation of the bifurcation sequences occurring in map T, in particular, related to routes involving the cycles mentioned above: the real fixed point, attracting 3-cycle and 4-cycle. We shall describe several bifurcation sequences, and the appearance/disappearance of cycles occurring in all the four kinds of transitions described above.

After this Introduction, the structure of the paper is as follows. In Sec. 2, we recall some properties of the map, the conditions for the invertibility, the fixed points, and the existence regions of a pair of 3-cycles and of 4-cycles. In Sec. 3, we shall consider two routes towards subcritical and supercritical center bifurcations, showing that bifurcations of the cases (A), (B) and (D) described above occur. In particular, examples of fold bifurcations leading to a pair of saddles. Moreover, the route to a subcritical bifurcation involves homoclinic loops and chaotic repellers. In Sec. 4, we shall consider three different routes associated with the 3-cycle. We shall describe the role played by bifurcations of the cases (A), (B) and (C) described above. In particular, examples of degenerate flip bifurcations of subcritical type, and the transition noninvertible/invertible, which is a route leading to multistability (coexistence of many attracting cycles). Section 5 concludes.

2. Preliminary Bifurcation Curves in the (a, c) Plane

Let us consider the two-dimensional PWL map given by $(x', y') = T(x, y)$ defined in (1) with $d = 1$ (without loss of generality), so that the system is a function of the two parameters (a, c). This PWL continuous map has a critical line LC_{-1} in $x = 0$. For our convenience, let us rewrite the system as follows:

$$T := \begin{cases} T_L(x, y) & \text{if } x \le 0, \\ T_R(x, y) & \text{if } x \ge 0, \end{cases} \tag{2}$$

where

$$T_L(x, y) := \begin{cases} x' = -x - ay, \\ y' = x - cy + 1, \end{cases}$$
$$T_R(x, y) := \begin{cases} x' = x - ay, \\ y' = x - cy + 1. \end{cases} \tag{3}$$

The regions $x > 0$ and $x < 0$ are called left/right partitions and the symbols R and L are used to denote the itinerary of a point and, in particular, the symbolic sequence of cycles.

Both functions T_L and T_R map the critical line $x = 0$ into the same line given, for $a \neq 0$, by

$$LC : \; y = \frac{c}{a}x + 1. \tag{4}$$

In this section we recall some properties and bifurcation curves reported in [Gardini & Tikjha, 2019], to be used for our analysis in the next sections.

A first property refers to the parameter values at which the map is invertible or noninvertible, leading to the following property:

(a) *for $c > 0$, map T is invertible for $a > c$, otherwise it is noninvertible of $Z_0 - Z_2$ type*;
(b) *for $c = a$, map T is degenerate, the half-plane $x > 0$ is mapped into the critical line LC ($y = x + 1$), thus it is noninvertible of $Z_0 - Z_1 - Z_\infty$ type*;

(c) *for $c < 0$, map T is invertible for $a > |c|$, otherwise it is noninvertible of $Z_0 - Z_2$ type;*

(d) *for $c = -a$, map T is degenerate, the half-plane $x < 0$ is mapped into the critical line LC $(y = -x + 1)$, thus it is noninvertible of $Z_0 - Z_1 - Z_\infty$ type.*

Recall that the main differences between invertible and noninvertible maps refer to the structure of invariant sets in the phase space. In invertible maps, homoclinic orbits can be related only to saddle cycles (intersection between the stable and unstable sets), and the basins of attracting sets are always simply connected. Differently, in noninvertible maps the homoclinic orbits can occur also for repelling nodes or foci (related to snap-back repellers) and the basins of attraction can also be multiply connected or disconnected. We shall see both cases described in the next sections.

The map has a unique fixed point which may be real:

$$P_L^* = (x_L^*, y_L^*) = \left(-\frac{a}{2+a+2c}, \frac{2}{2+a+2c}\right) \quad (5)$$

since $P_R^* = (x_R^*, y_R^*) = (-1, 0)$ having $x_R^* < 0$ is always virtual. Differently, P_L^* is a real fixed point of map T for $a > 0$ and $c > -1 - \frac{a}{2}$ or $a < 0$, and $c < -1 - \frac{a}{2}$. The stability analysis depends on the eigenvalues of the Jacobian matrix, having $\mathrm{tr}(J_R) = (1 - c)$ and $D_R = \det(J_R) = (a - c)$ so that the characteristic polynomial $\mathcal{P}_R(\lambda)$ leads to $\mathcal{P}_R(1) = a$, $\mathcal{P}_R(-1) = 2 + a - 2c$ and the region in the (a, c) parameter plane in which it is a virtual attracting fixed point, given by $\mathcal{P}_R(1) > 0$, $\mathcal{P}_R(-1) > 0$ and $D_R < 1$, is given by $S_R^* := \{a > 0,\ c < \frac{a}{2} + 1,\ c > a - 1\}$. For the real fixed point P_L^*, since $\mathrm{tr}(J_L) = -(1 + c)$ and $D_L = \det(J_L) = (a + c)$, the characteristic polynomial $\mathcal{P}_L(\lambda)$ leads to $\mathcal{P}_L(-1) = a$, $\mathcal{P}_L(1) = 2 + a + 2c$ and the region in the (a, c) parameter plane in which $\mathcal{P}_L(1) > 0$, $\mathcal{P}_L(-1) > 0$ and $D_L < 1$ hold is given by

$$S_L^* := \left\{a > 0,\ c > -\frac{a}{2} - 1,\ c < -a + 1\right\}. \quad (6)$$

Clearly the borders of the regions correspond to bifurcations of the fixed point. $\mathcal{P}_L(-1) = 0$ to a degenerate flip, $\mathcal{P}_L(1) = 0$ to a degenerate transcritical and $D_L = 1$ to a center bifurcation, which has been shown to be supercritical for $c > 0$ and subcritical for $c < 0$.

The existence region of the real fixed point P_L^* is shown colored in the (a, c) parameter plane in Fig. 1(a), and in the bright yellow triangle P_L^* is attracting. In the same figure we have also reported the boundaries of the stability region of the virtual fixed point P_R^* to prove when it is attracting or repelling.

The existence of an attracting virtual fixed point P_R^*, or a repelling focus, implies that the trajectories from the right partition are always mapped in the left partition in a finite number of iterations. This creates the possibility to have attracting cycles with periodic points in both partitions, coexisting with the attracting fixed point P_L^*. And in fact, in map T we have an existence region of a pair of 3-cycles, which overlaps with that of the fixed point

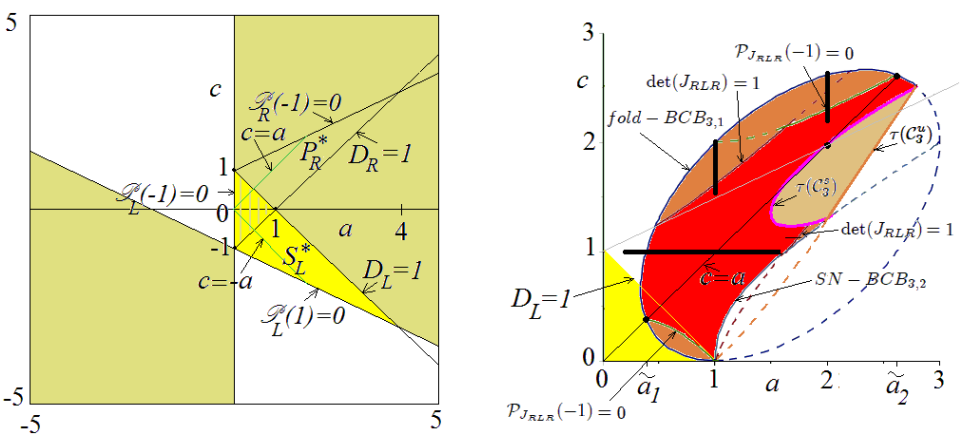

(a) (b)

Fig. 1. In (a) the existence and stability regions of the fixed points in the (a, c) parameter plane are evidenced. In (b) the existence and stability region of a pair of 3-cycles is evidenced. The paths in black will be considered in Sec. 4.

P_L^*, and in part with the stability region of P_L^*. In [Gardini & Tikjha, 2019] the existence region of a 3-cycle of map T is obtained looking for the solutions of the equation $T^3(x,y)=(x,y)$ noting that the symbolic sequence of the two cycles are RLR and RLL and when they are merging we have RLC denoting with C a point on the critical line LC_{-1}. Considering $T_R\circ T_L\circ T_R(x,y)$ where

$$T_R\circ T_L\circ T_R(x,y) = \begin{bmatrix} (ac-2a-1) & (ac+a-ac^2+a^2) \\ (-a-c+c^2+1) & (a+2ac-c^3) \end{bmatrix}\begin{bmatrix} x \\ y \end{bmatrix} + \begin{bmatrix} -2a+ac \\ -a-c+c^2+1 \end{bmatrix}, \quad (7)$$

a periodic point of a real 3-cycle $\mathcal{C}_3^s$ which may be attracting is given by

$$(x_{3,1}^s, y_{3,1}^s) = \left(\frac{a(-c^2-a^2+ac+2a+c-1)}{2c^3+a^3-a^2c-c^2a-3ac+a+2}, \frac{2(c^2-c-ac+a+1)}{2c^3+a^3-a^2c-c^2a-3ac+a+2}\right). \quad (8)$$

While considering

$$T_L\circ T_R\circ T_L(x,y) = \begin{bmatrix} 2a+1+ac & -c^2a-ac+a^2+a \\ c-a+c^2-1 & 2ac-a-c^3 \end{bmatrix}\begin{bmatrix} x \\ y \end{bmatrix} + \begin{bmatrix} ac \\ c^2-a-c+1 \end{bmatrix} \quad (9)$$

and solving for $T_L\circ T_R\circ T_L(x,y)=(x,y)$ a periodic point $(x_{3,1}^u, y_{3,1}^u)$ of a real 3-cycle $\mathcal{C}_3^u$ (which is repelling) is obtained, given by

$$(x_{3,1}^u, y_{3,1}^u) = \left(\frac{-(a^2-ac+c-c^2-1)}{a^2+ac-3c-c^2-1}, \frac{2(a-1)}{a^2+ac-3c-c^2-1}\right). \quad (10)$$

The two 3-cycles appear/disappear via fold-BCB at a parameter point (a,c) for which it is $x_{3,1}^s=0$, and for $a\neq 0$ this leads to the necessary condition

$$\text{fold-BCB}_{3,1}:\ c^2+a^2-ac-2a-c+1=0 \quad (11)$$

and another fold border collision bifurcation occurs considering the numerator of $x_{3,1}^u$ in (10), for

$$\text{fold-BCB}_{3,2}:\ a^2-ac+c-c^2-1=0. \quad (12)$$

The existence region of the pair of 3-cycles is also bounded by a curve related to a degenerate transcritical bifurcation occurring when one eigenvalue becomes 1 and the periodic points of the cycles tend to infinity. For the 3-cycle $\mathcal{C}_3^s$ this occurs when the parameter point (a,c) belongs to the curve denoted by $\tau(\mathcal{C}_3^s)$:

$$\tau(\mathcal{C}_3^s):\ 2c^3+a^3-a^2c-c^2a-3ac+a+2=0 \quad (13)$$

while for the other 3-cycle saddle $\mathcal{C}_3^u$ the degenerate transcritical bifurcation occurs for:

$$\tau(\mathcal{C}_3^u):\ a^2+ac-3c-c^2-1=0. \quad (14)$$

These curves are shown in Fig. 1(b). Inside the existence region, the stability region of $\mathcal{C}_3^s$ is bounded by bifurcation curves related to the center bifurcations and degenerate flip bifurcations, so that these can be determined from the eigenvalues of the function $T_R\circ T_L\circ T_R(x,y)$, for which we have $\text{tr}(J_{RLR})=3ac-c^3-a-1$ and $\det(J_{RLR})=(a-c)^2(a+c)$. The stability conditons are $\mathcal{P}_{J_{RLR}}(1)=2c^3+a^3-a^2c-c^2a-3ac+a+2>0$, $\mathcal{P}_{J_{RLR}}(-1)=a(a^2-c^2-ac+3c-1)>0$ and $\det(J_{RLR})<1$ leading to the red portion shown in Fig. 1(b).

As mentioned in the Introduction, when a parameter point belongs to the degenerate transcritical bifurcation curves we also have the related Jacobian matrix with one eigenvalue +1. Other bifurcations of the cycles are related to the eigenvalues of the map T^3.

Two small arcs of the fold-BCB curve in (11) are related to the appearance of an attracting node and a saddle, the other two arcs are related to the appearance of two unstable 3-cycles. The bifurcation curves obtained from the stability conditions $\mathcal{P}_{J_{RLR}}(-1)=0$ and $\det(J_{RLR})=1$ bound the stability region in two different parts. A numerical investigation has shown that the portion of $\mathcal{P}_{J_{RLR}}(-1)=0$ in the lower region (associated with an attracting fixed point) is related to a degenerate flip-BCB of subcritical type (attracting 6-cycles merge with LC_{-1} at the bifurcation of a saddle 3-cycle with an eigenvalue equal to -1, leading to an attracting 3-cycle), while the portion in the upper part is related to a supercritical one (an attracting 3-cycle undergoes a bifurcation with an eigenvalue equal to -1, becoming a saddle and leading to an attracting 6-cycle). Similarly for the center bifurcation curve ($\det(J_{RLR})=1$), there are two portions belonging to the existence region. The lower one

is in a region in which the map is invertible and related to a center bifurcation of subcritical type, while the upper one is in a region of noninvertibility and the center bifurcation is supercritical.

Differently, for the 3-cycle $\mathcal{C}_3^u$, from the Jacobian matrix J_{LRL} in Eq. (9) we have $\mathcal{P}_{J_{LRL}}(1) = a^2 + ac - 3c - c^2 - 1$ and $\mathcal{P}_{J_{LRL}}(1) > 0$ is the region below the curve $\tau(\mathcal{C}_3^u)$, so that for any (a, c) belonging to the existence region of the cycle $\mathcal{C}_3^u$, one real eigenvalue is always greater than 1 (being $\mathcal{P}_{J_{LRL}}(1) < 0$).

As it can be seen from Fig. 1(b), there is an overlapping between the stability region of the fixed point P_L^* with the existence region of the 3-cycles, in particular, with a region in which both 3-cycles are unstable and a region in which the 3-cycle $\mathcal{C}_3^s$ is attracting. In Sec. 4, we shall come back to comment on the dynamics when the parameters are crossing the stability region of the 3-cycle, along the black paths evidenced in Fig. 1(b), increasing c along $a = 1$ crossing a supercritical center bifurcation, and increasing c along $a = 2$ crossing a degenerate flip bifurcation, and describing the changes occurring in the transition noninvertible/invertible increasing a along $c = 1$.

Let us first recall some bifurcations related to 4-cycles. Consider the function $T_R^2 \circ T_L \circ T_R(x, y)$:

$$\begin{bmatrix} 2ac - ac^2 + a^2 - 1 - a & -2a^2c + ac + ac^3 - ac^2 + a \\ 2ac + c^2 - c^3 - 2a + c - 1 & a^2 - 3ac^2 + a + c^4 \end{bmatrix} \begin{bmatrix} x \\ y \end{bmatrix} + \begin{bmatrix} -ac^2 + 2ac - 3a + a^2 \\ c^2 - c + 1 - 2a + 2ac - c^3 \end{bmatrix}$$

and looking for its fixed point (a periodic point with symbolic sequence $RLRR$), we get

$$\begin{aligned} x_{4,1}^s &= \frac{a(-a^3 + 2c^3 + 2a^2c - 2ac^2 + 2a^2 - 2c^2 - 4ac + 2a + 2c - 2)}{a^4 - 2c^4 - 2a^3c + 2ac^3 + 4ac^2 - 2a^2 - 2ac + 2}, \\ y_{4,1}^s &= \frac{2(1-c)((a-c)^2 + 1)}{a^4 - 2c^4 - 2a^3c + 2ac^3 + 4ac^2 - 2a^2 - 2ac + 2}, \end{aligned} \tag{15}$$

which results in the periodic point of a 4-cycle $\mathcal{C}_4^s$ which can be attracting, appearing via fold-BCB crossing through an arc of the curve of equation

$$\text{fold-BCB}_{4,1}: \quad \frac{1}{2}a^3 - c^3 - a^2c + ac^2 - a^2 + c^2 + 2ac - c - a + 1 = 0 \tag{16}$$

obtained from $x_{4,1}^s = 0$, for $a \neq 0$, and bounding the blue colored existence region in Fig. 2(a), related to a pair of 4-cycles, a saddle and an attracting node. The repelling 4-cycle saddle, say $\mathcal{C}_4^u$, appearing at the fold-BCB has symbolic sequence $LLRR$, and a point of this cycle is obtained considering the fixed point

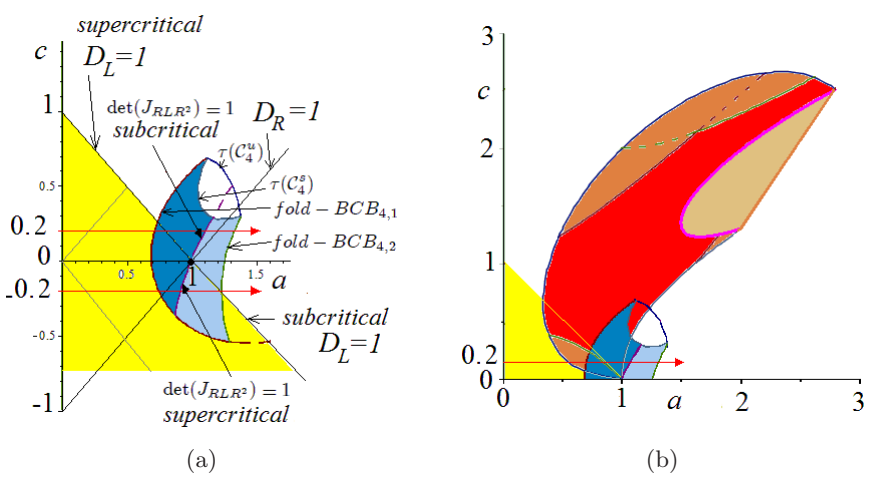

Fig. 2. In (a) existence and stability regions of the 4-cycles in the (a, c) parameter plane. In the blue colored area the 4-cycle C_4^s is attracting. The two paths in red are considered in Sec. 3. In (b) the existence regions of the 3-cycles and 4-cycles are both shown, overlapped with the stability region of the fixed point P_L^* for $c > 0$.

of the function $T_R^2 \circ T_L^2(x,y)$, leading to

$$x_{4,1}^u = \frac{-(a^3 - 2c^3 - 2a^2c + 2ac^2 - 2a^2 + 2c^2 + 4ac - 2a - 2c + 2)}{a^3 - 2ac^2 + 4c^2 - 2a},$$

$$y_{4,1}^u = \frac{2((a-c)^2 + 2c - a - 1)}{a^3 - 2ac^2 + 4c^2 - 2a}.$$

The stability of the 4-cycle $\mathcal{C}_4^s$ can be determined considering the Jacobian matrix J_{RLR^2} and its trace and determinant, that is:

$$\begin{aligned} &\mathrm{tr}(J_{RLR^2}) = 2ac - 4ac^2 + 2a^2 - 1 + c^4 \quad \text{and} \\ &\det(J_{RLR^2}) = (a-c)^3(a+c). \end{aligned} \tag{17}$$

The stability region in the parameter plane is the one in which we have satisfied the three conditions $\mathcal{P}_{J_{RLR^2}}(1) = a^4 - 2c^4 - 2a^3c + 2ac^3 + 4ac^2 - 2a^2 - 2ac + 2 > 0$, $\mathcal{P}_{J_{RLR^2}}(-1) = 2ac - 4ac^2 + 2a^2 - 2a^3c + 2ac^3 + a^4 > 0$ and $\det(J_{RLR^2}) = (a-c)^3 \times (a+c) < 1$, and it is colored in Fig. 2(a) in dark blue, while the azure color denotes 4-cycles both repelling. The separation curve is related to a center bifurcation occurring at $\det(J_{RLR^2}) = 1$, which has been shown to be subcritical for $c > 0$ and supercritical for $c < 0$.

The lower boundary of this azure region (bounding the existence region) is another fold-BCB in which the periodic point with symbolic sequence R^3L (of a repelling node) and the periodic point with symbolic sequence LR^2L (of a saddle) are merging. Considering the function $T_L \circ T_R^3(x,y)$ and looking for its fixed point, we get

$$x_{4,1}^n = \frac{a(-a^3 - 2c^3 + 2a^2c + 2c^2 - 2c + 2)}{a^4 - 2c^4 - 2a^3c + 2ac^3 + 4ac^2 - 2a^2 - 2ac + 2},$$

$$y_{4,1}^n = \frac{2(1-c)(c^2 - 2a + 1)}{a^4 - 2c^4 - 2a^3c + 2ac^3 + 4ac^2 - 2a^2 - 2ac + 2}$$

and the fold-BCB (in which a 4-cycle saddle and a repelling node are merging on $x = 0$) occurs at parameter points belonging to the curve obtained from $x_{4,1}^n = 0$, for $a \neq 0$:

$$\text{fold-BCB}_{4,2}\colon \quad a^3 + 2c^3 - 2a^2c - 2c^2 + 2c - 2 = 0. \tag{18}$$

The existence region of both 4-cycles $\mathcal{C}_4^s$ and $\mathcal{C}_4^u$ is bounded by degenerate transcritical bifurcations of the two cycles, occurring for the attracting cycle when

$$\tau(\mathcal{C}_4^s)\colon \ \mathcal{P}_{J_{RLR^2}}(1) = a^4 - 2c^4 - 2a^3c + 2ac^3 + 4ac^2 - 2a^2 - 2ac + 2 = 0 \tag{19}$$

and for the unstable one when

$$\tau(\mathcal{C}_4^u)\colon \ \mathcal{P}_{J_{L^2R^2}}(1) = a^3 - 2ac^2 + 4c^2 - 2a = 0 \tag{20}$$

whose interesting arcs are shown in Fig. 2(a).

As for the pair of 3-cycles, we observe that also the existence region of the pair of 4-cycles overlaps with the stability triangle of P_L^* (in which also the virtual fixed point P_R^* is attracting). Moreover, in Fig. 2(b) we overlap for $c > 0$ (when the pair of 3-cycles exist) the considered existence region of the pair of 4-cycles, so that it can be seen, in particular, the overlapping of the stability regions of three coexisting different attractors.

In the next section we shall describe some bifurcations related to the cycles determined in this section, increasing the parameter a along the lines $c = -0.2$ and $c = 0.2$.

3. Bifurcation Sequences Related to the Center Bifurcation of $\mathcal{C}_4^s$

In this section, we describe some bifurcations, or transitions, showing how the dynamics are modified reaching the bifurcation values of the 4-cycle $\mathcal{C}_4^s$ and of the fixed point P_L^*. Since such dynamics and bifurcations are relevant in the considered piecewise linear system, we shall describe in two different subsections the dynamics occurring for $c = -0.2$ fixed and $c = 0.2$ fixed, increasing the parameter a, along the paths indicated in Fig. 2(a) with two horizontal arrows. These are representative of the bifurcations occurring in the two cases $c < 0$ and $c > 0$. In fact, the same kind of bifurcations of the 4-cycle $\mathcal{C}_4^s$ occur whenever the center bifurcation curve is crossed for $c > 0$ or $c < 0$. Notice that the values of center bifurcation curve of $\mathcal{C}_4^s$ belong to the parameter region in which the map is uniquely invertible. In the routes described below, we shall see examples of the cases (A), (B) and (D) mentioned in

the Introduction, as well as the homoclinic tangles associated with a subcritical center bifurcation.

3.1. *Towards a supercritical center bifurcation of $\mathcal{C}_4^s$ and subcritical of P_L^**

Let us here consider $c = -0.2$ fixed, so that close to the center bifurcation the virtual fixed point P_R^* is a repelling focus. We know that increasing a, the 4-cycle undergoes a supercritical center bifurcation while P_L^* undergoes a subcritical center bifurcation, so we are interested in this transition in order to show how these two center bifurcations are reached.

Increasing the parameter a, the attracting fixed point P_L^* will coexist with other attracting cycles. At $a \simeq 0.743562$ a fold-BCB (case (A)) leads to the appearance of the pair of 4-cycles described in Sec. 2, one of which is an attracting node, and one a saddle, whose stable set separates the basins $\mathcal{B}(\mathcal{C}_4^s)$ and $\mathcal{B}(P_L^*)$. An example is shown in Fig. 3(a). Moreover, we have observed that this 4-cycle is not the unique coexisting attracting cycle. In fact, increasing the parameter a, before the occurrence of the center bifurcation of $\mathcal{C}_4^s$, at $a \simeq 0.91718134$, one more attracting cycle appears (always via fold-BCB, case (A)), an attracting 9-cycle $\mathcal{C}_9^s$ in pair with a saddle 9-cycle. Three coexisting attractors are shown in Fig. 3(b), the 4-cyclic attracting closed invariant curves (attracting set existing after the supercritical center bifurcation of $\mathcal{C}_4^s$, case (D)), the 9-cycle $\mathcal{C}_9^s$ and the fixed point P_L^*. The basin of attraction of the 4-cyclic closed invariant curves is bounded by the stable set of the saddle cycle $\mathcal{C}_4^u$ and the curves are far from the boundary (and thus also at the value of center bifurcation of $\mathcal{C}_4^s$ the invariant regions tangent to $x = 0$ are far from the basin boundary). Increasing the parameter a the closed curves are increasing in size, approaching the basin boundary. Notice that a contact of the 4-cyclic closed invariant curves with the stable set of the saddle $\mathcal{C}_4^u$ bounding the basin will lead to the disappearance of the attractor via homoclinic bifurcation of the saddle $\mathcal{C}_4^u$, this is illustrsted in Fig. 4(a), where the chaotic transient is shown, before convergence to the fixed point P_L^*, coexisting with the attracting 9-cycle $\mathcal{C}_9^s$. Also this attracting 9-cycle $\mathcal{C}_9^s$ undergoes a center bifurcation (case (D)) for $a \simeq 0.9527$, and we can predict that it is of supercritical type. In fact, the symbolic sequence of the attracting 9-cycle has six points in the right partition and three in the left one, so that before the center bifurcation, it is $0 < D_{R^6L^3} = (a-c)^6(a+c)^3 < 1$, while the symbolic sequence of the saddle 9-cycle has five points in the right partition and four in the left one, so that it is $0 < D_{R^5L^4} = (a-c)^5(a+c)^4 < D_{R^6L^3} < 1$, which means that map T^9 cannot have repelling nodes, so that before the bifurcation a repelling closed curve (connection saddle-repelling node) cannot exist.

An example of 9-cyclic attracting closed invariant curves coexisting with the fixed point P_L^*, is shown in Fig. 4(b), and increasing the value of a here the disappearance of the attracting set occurs via contact bifurcation when the 9-cycle saddle becomes homoclinic, leaving the fixed point P_L^*

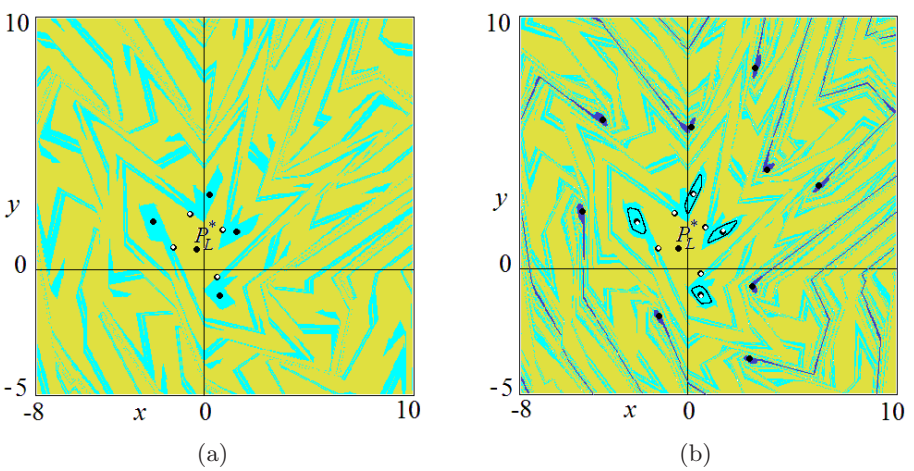

Fig. 3. In (a) $a = 0.91$, $c = -0.2$, phase space showing the basin $B(P_L^*)$ in yellow and the basin $B(C_4^s)$ in azure, separated by the stable set of the saddle C_4^u. In (b), $a = 0.925$, $c = -0.2$, phase space after the supercritical center bifurcation of C_4^s, showing the basin $B(P_L^*)$ in yellow, the basin of the closed attracting curves in azure, separated by the stable set of the saddle C_4^u, and the basin of an attracting 9-cycle in blue, bounded by the stable set of a saddle 9-cycle.

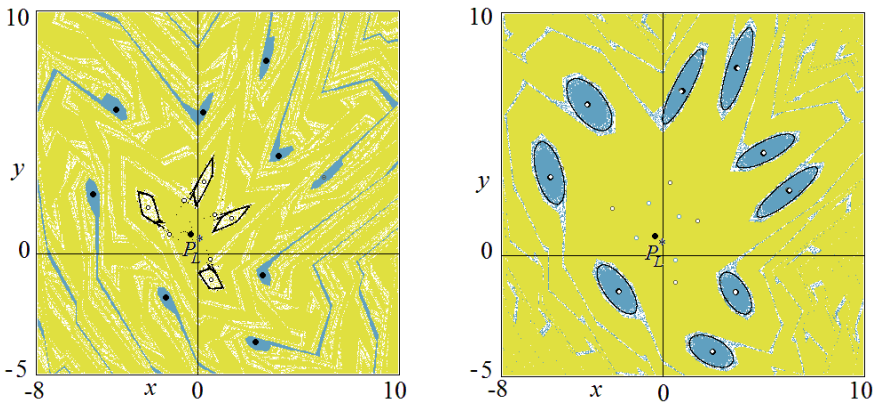

Fig. 4. In (a), $a = 0.93$, $c = -0.2$, phase space showing the basin $B(P_L^*)$ in yellow and the basin of an attracting 9-cycle in blue, the saddle C_4^u is homoclinic after the contact of the closed attracting curves with their immediate basin boundary. In (b), $a = 0.9527$, $c = -0.2$, phase space showing the basin $B(P_L^*)$ in yellow and the basin of attraction of closed curves in blue after the center bifurcation of an attracting 9-cycle, separated by the stable set of a saddle 9-cycle, and a chaotic repeller associated with the homoclinic 4-cycle saddle exists.

as unique attractor. However, it is evident that a chaotic repeller exists in the phase plane, due to the existence of homoclinic orbits.

Increasing the parameter a, towards the subcritical center bifurcation of the fixed point, divergent trajectories are also observed. In Fig. 5(a) the basin of attraction of P_L^* is bounded by the stable set of the saddle cycle $\mathcal{C}_4^u$ which is homoclinic on one side. There exists one branch of unstable set of $\mathcal{C}_4^u$ which is convergent to P_L^* without intersecting its stable set. However, also this branch will become homoclinic, and the basin boundary of $\mathcal{B}(P_L^*)$ becomes a closed repelling invariant curve approaching the bifurcation value. The subcritical center bifurcation, at $a = 1.2$, is shown in Fig. 5(b).

It is worth noting that also after this bifurcation value, not all the trajectories are divergent, for example, besides the unstable fixed point P_L^*, the pair of unstable 4-cycles exists up to their disappearance by fold-BCB at $a \simeq 1.2354$.

3.2. *Towards a subcritical center bifurcation of $\mathcal{C}_4^s$ and supercritical of P_L^**

Let us here consider $c = 0.2$ fixed, so that the virtual fixed point P_R^* is attracting up to $a = 0.8$, and we have already shown in Sec. 2 that in this range at least two more attracting cycles appear, a 3-cycle $\mathcal{C}_3^s$ and a 4-cycle $\mathcal{C}_4^s$, coexisting with the attracting

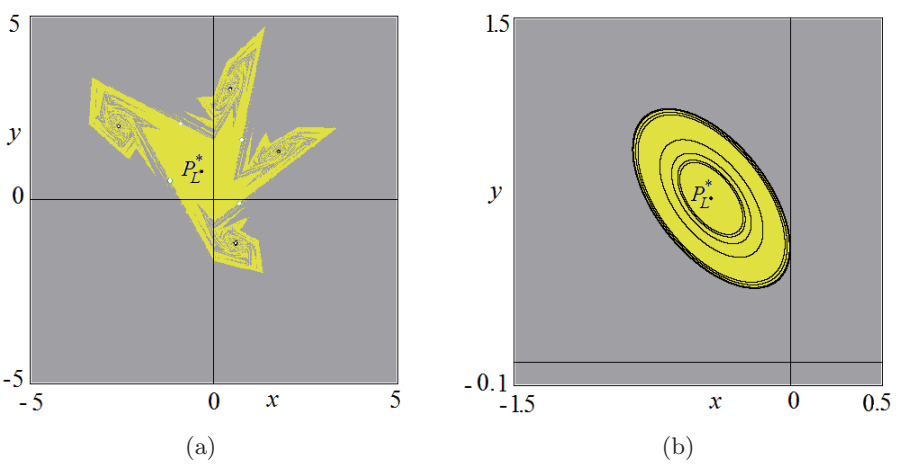

Fig. 5. In (a), $a = 1$, $c = -0.2$, phase space showing the basin $B(P_L^*)$ in yellow and the region of divergent trajectories in gray, separated by the stable set of the saddle 4-cycle C_4^u, which is homoclinic on one side. In (b) $a = 1.2$, $c = -0.2$, subcritical center bifurcation of P_L^*.

fixed point P_L^*. Increasing the parameter, the fixed point P_L^* is attracting and at $a \simeq 0.4917237$ a fold-BCB leads to the appearance of a pair of 3-cycles, and both are unstable. This is a peculiarity of the case (A): that is, this is an example of fold-BCB which leads to the appearance of a pair of saddle cycles. The saddle with symbolic sequence RLL has two real and positive eigenvalues, while the saddle with symbolic sequence RLR has two real and negative eigenvalues. This second saddle cycle is related to the existence of a two-piece chaotic attractor. That is, this bifurcation leads also to the appearance of a new attracting set: six chaotic segments, say $\mathcal{A}_6$, since they are related to a repelling 3-cycle saddle while the stable set of the second saddle 3-cycle separates the basins $\mathcal{B}(\mathcal{A}_6)$ and $\mathcal{B}(P_L^*)$.

This occurs up to the appearance of the pair of 4-cycles, at $a \simeq 0.71559164$, leading to an attracting 4-cycle node ($\mathcal{C}_4^s$) and a saddle 4-cycle ($\mathcal{C}_4^u$) whose stable set bounds the basin $\mathcal{B}(\mathcal{C}_4^s)$. Increasing a, the chaotic set $\mathcal{A}_6$ becomes an attracting 6-cycle, and one more attractor appears by fold-BCB, an attracting 18-cycle (case (A) leading to an attracting cycle and a saddle). This leads to four coexisting attracting sets, as shown in Fig. 6, where the value of the parameter is very close to the bifurcation value $a \simeq 0.77082$, at which the 6-cycle undergoes a degenerate subcritical flip bifurcation. In fact, in the enlargement shown in Fig. 6(b) we see that the 6-cycle is close to the critical line $x = 0$ and at this subcritical flip (of the 3-cycle), the 6-cycle disappears while the 3-cycle $\mathcal{C}_3^s$ becomes an attracting node (case (B) subcritical of the 3-cycle). Also the 18-cycle is very close to the border $x = 0$, and in fact it will also undergo a degenerate subcritical flip bifurcation leading to an attracting 9-cycle node (case (B) subcritical of the 9-cycle), as shown in Fig. 7.

Then the 9-cycle disappears via fold-BCB together with a saddle 9-cycle (case (A)) and the attracting fixed point is close to its center bifurcation (case (D)), occurring at $a = 0.8$, leading to an attracting invariant closed curve Γ_+, as shown in Fig. 8(a). A contact between the invariant attracting set related to the supercritical center bifurcation of P_L^* with the frontier of its basin boundary, given by the stable set of the saddle 3-cycle $\mathcal{C}_3^u$, will leave only two attractors, $\mathcal{C}_4^s$ and $\mathcal{C}_3^s$, whose basins are separated by the stable set of the saddle $\mathcal{C}_4^u$.

Notice that after such contact bifurcation the stable set of the saddle $\mathcal{C}_3^u$ separates the basins of the three fixed points for the cubic iterate of the map, T^3, as shown in Fig. 8(b) and has a fractal structure, since the saddle 3-cycle is homoclinic.

Increasing the parameter a, at $a \simeq 1.082888$ the pair of 3-cycles disappears via fold-BCB, leaving the attracting 4-cycle as attracting set in a neighborhood of P_L^*. However, it is not the unique attracting set in the phase plane. In fact, for $a > \sqrt{1.04} \simeq 1.0198$ it is $D_L D_R > 1$ and thus the stable set of the 4-cycle saddle may not be issuing from infinity since several pairs of cycles may appear via

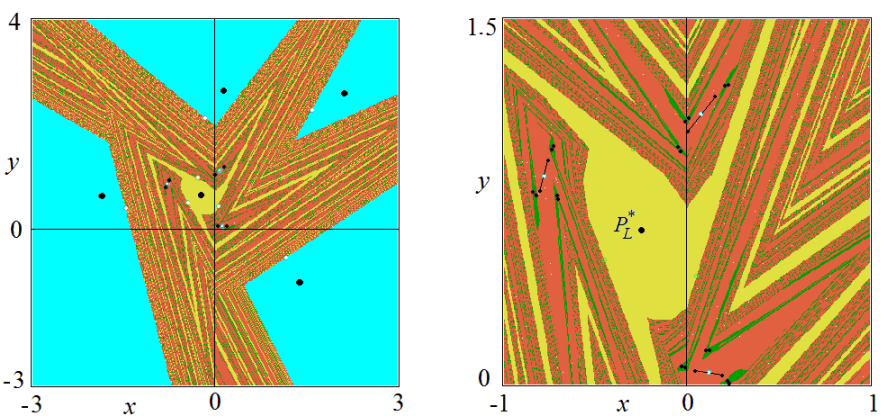

(a) (b)

Fig. 6. In (a), $a = 0.77$, $c = 0.2$, phase space showing four coexisting attractors: the basin $B(P_L^*)$ in yellow, the basin of an attracting 6-cycle in red, separated by the stable set of the saddle C_3^u, the basin of an attracting 18-cycle in green, bounded by the stable set of a saddle 9-cycle and the basin $B(C_4^s)$ in azure bounded by the stable set of the saddle C_4^u. In (b) enlargement around P_L^* showing that the attracting 6-cycle is close to a border collision bifurcation, one periodic point is close to LC_{-1}, and also the 18-cycle is close to a border collision. Both border collisions are related to a subcritical degenerate flip bifurcation, of a 3-cycle and of a 9-cycle, respectively.

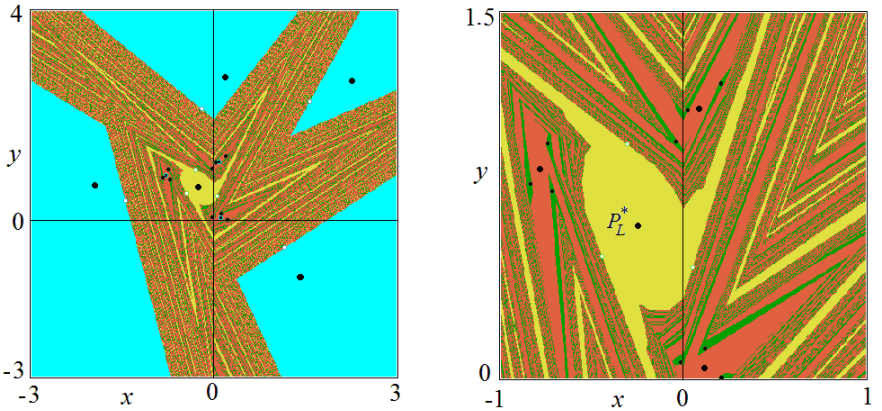

(a) (b)

Fig. 7. In (a), $a = 0.78$, $c = 0.2$, phase space after the subcritical flip bifurcations, showing four coexisting attractors: the basin $B(P_L^*)$ in yellow, the basin of the attracting 3-cycle C_3^s in red, separated by the stable set of the saddle C_3^u, the basin of an attracting 9-cycle in green, bounded by the stable set of a saddle 9-cycle and the basin $B(C_4^s)$ in azure, bounded by the stable set of the saddle C_4^u. In (b) enlargement around P_L^* showing the periodic points of the 3-cycle and of the 9-cycle.

fold-BCB, in particular, at $a = 1.08$ the 4-cycle coexists with a 21-cycle. Moreover, divergent trajectories may occur (i.e. the Poincaré Equator of the real phase plane may become attracting). An example is shown in Fig. 9(a) where the basins of the attracting 4-cycle and 21-cycle are colored (in azure and green, respectively), and gray points denote the existence of divergent trajectories, and the white areas prove the existence of several other attracting cycles. But of interest is the stable set of the saddle 4-cycle $\mathcal{C}_4^u$, which is now bounded, it is not reaching infinity: its limit set is a repelling closed invariant curve, as shown in the enlargement in Fig. 9(b) where the basin of the attracting 4-cycle is considered for map T^4 by using four different colors: the boundary of these regions is the stable set of the saddle 4-cycle $\mathcal{C}_4^u$.

The occurrence of invariant repelling closed curves, existing in the cases of a subcritical center bifurcation, is related to homoclinic tangles of the saddle cycles (a mechanism which is nowadays well known). Let us observe the one occurring here, related to the attracting 4-cycle $\mathcal{C}_4^s$ and the 4-cycle saddle $\mathcal{C}_4^u$ bounding its basin of attraction. In Fig. 10, we show an enlargement evidencing in particular one point of the saddle 4-cycle. In Fig. 10(a)

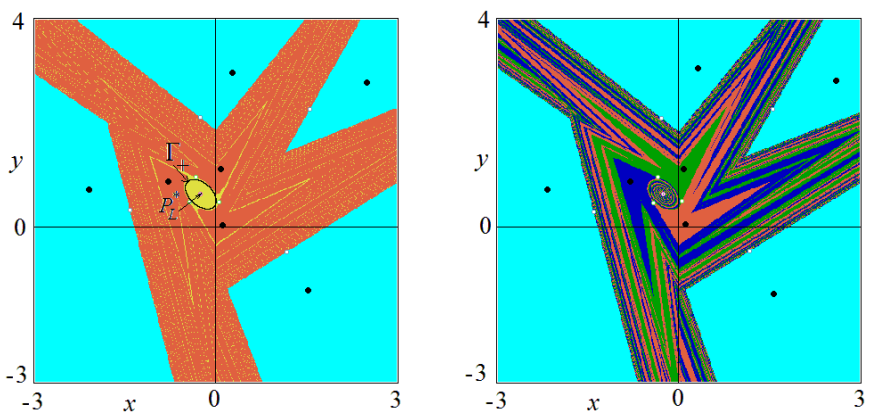

(a) (b)

Fig. 8. In (a), $a = 0.8005$, $c = 0.2$, phase space after the supercritical center bifurcation of P_L^* showing three coexisting attractors: the basin of an attracting closed curve Γ_+ in yellow, the basin of the attracting 3-cycle C_3^s in red, separated by the stable set of the saddle C_3^u and the basin $B(C_4^s)$ in azure, bounded by the stable set of the saddle C_4^u. In (b) $a = 0.81$, $c = 0.2$, phase space after the disappearance of the attracting closed curve Γ_+, leaving only two attractors. The basin of the attracting 3-cycle C_3^s is shown for map T^3 separated by the stable set of the saddle C_3^u which has a complex structure. The basin $B(C_4^s)$, bounded by the stable set of the saddle C_4^u is in azure.

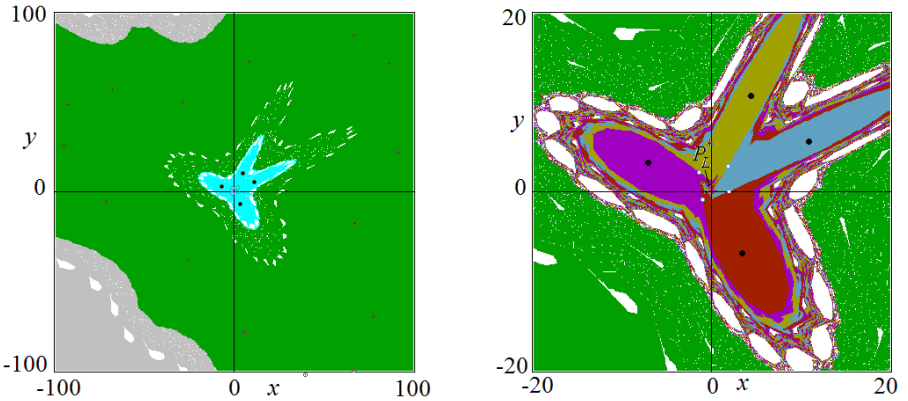

(a) (b)

Fig. 9. In (a), $a = 1.09$, $c = 0.2$, phase space showing different attracting sets. The basin $B(C_4^s)$ in azure, the basin of an attracting cycle of period-21 in green, divergent trajectories in gray, regions related to other attracting cycles of different periods in white. In (b) enlargement around P_L^*, showing the basins of the four fixed points of C_4^s for map T^4, with four different colors, separated by the stable set of the saddle C_4^u which is now a bounded invariant set.

the stable set is still non-homoclinic, but it is evident that the stable set is approaching one branch of the unstable set, that is, approaching homoclinic orbits. Recall that in invertible maps, transverse homoclinic orbits of saddle cycles are always related to invariant chaotic sets. In Fig. 10(b) the stable set separates bounded orbits from divergent ones, and one branch of the unstable set of the saddle 4-cycle of T is homoclinic (some points are convergent to the attracting 4-cycle and some points are diverging). In Fig. 10(c) one branch of the unstable set of the saddle 4-cycle is completely included in the region of divergent trajectories, while the opposite branch converges to the attracting 4-cycle, the stable set separates the four regions and the homoclinic bifurcation of the second unstable branch is approaching.

In Fig. 11(a) the stable and unstable sets of the saddle are intersecting, that is, we are inside the homoclinic loop, which already ended in Fig. 11(b): the stable and unstable sets of the saddle $\mathcal{C}_4^u$ are now no longer related to the attracting 4-cycle $\mathcal{C}_4^s$ as it is better visible in Fig. 11(c).

The center bifurcation of the attracting 4-cycle $\mathcal{C}_4^s$ occurring at $a \simeq 1.1131837$, of subcritical type, is approached, as shown in Fig. 12(a), where the gray points denote divergent trajectories, and four closed invariant repelling curves bound the basin

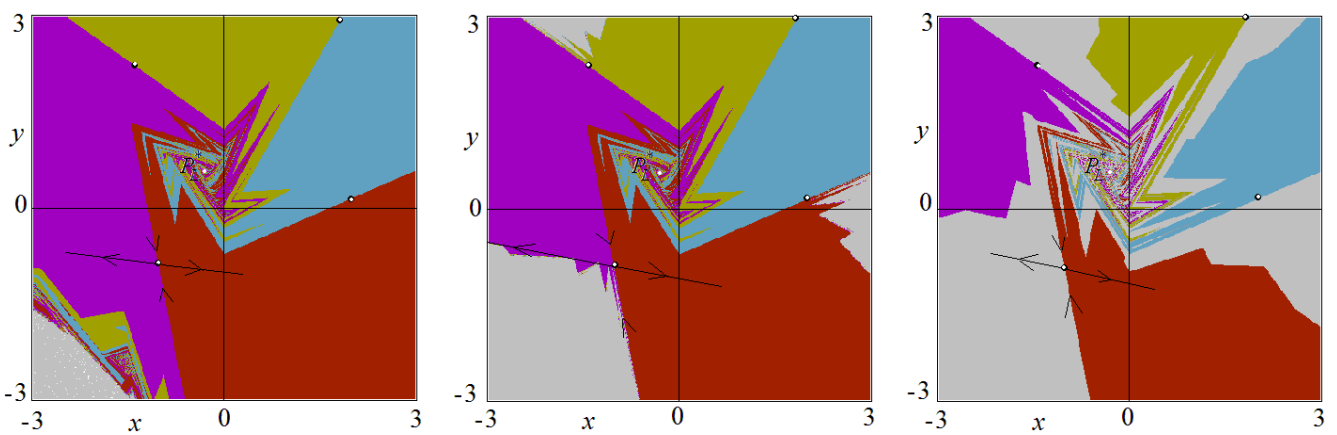

(a) (b) (c)

Fig. 10. Bifurcation sequence at $c = 0.2$, showing an enlargement of the phase space around P_L^*, with the basins of the four fixed points of C_4^s for map T^4 in four different colors, separated by the stable set of the saddle C_4^u, while gray points denote divergent trajectories. In (a) $a = 1.095$, the saddle C_4^u is not homoclinic. In (b) $a = 1.1$, the saddle C_4^u is homoclinic on one side, some points of the unstable set have divegent trajectories. In (c) $a = 1.104$, the saddle C_4^u is close to the homoclinic bifurcation of the second unstable branch.

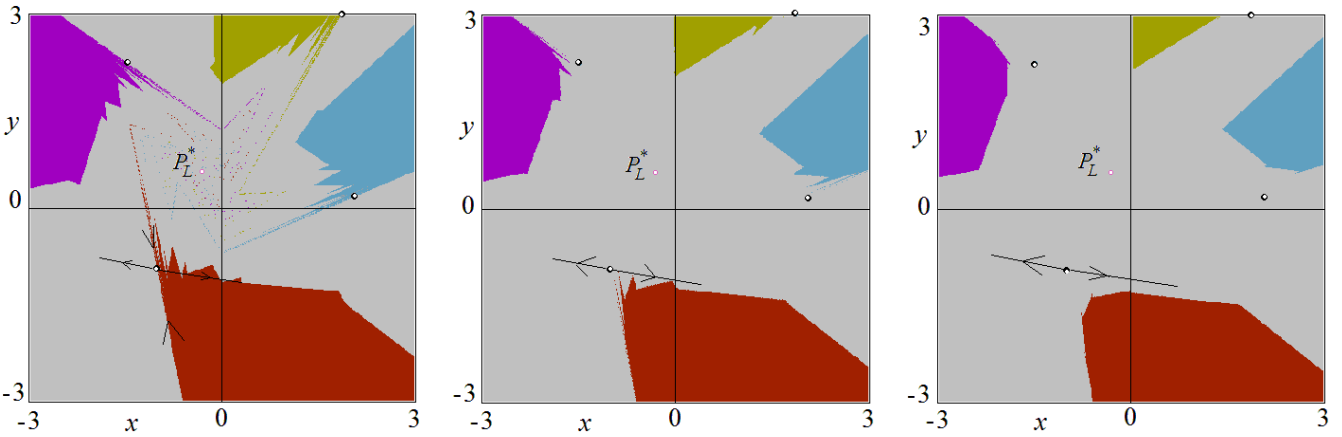

Fig. 11. Bifurcation sequence at $c = 0.2$, showing an enlargement of the phase space around P_L^*, with the basins of the four fixed points of C_4^s for map T^4 in four different colors. In (a) $a = 1.1075$, the saddle C_4^u is homoclinic on both sides, and the stable set belongs to the basin boundary of C_4^s. In (b) at $a = 1.1086$ and in (c) at $a = 1.1091$, the saddle C_4^u is homoclinic and the stable set is not related to the basin boundary of C_4^s.

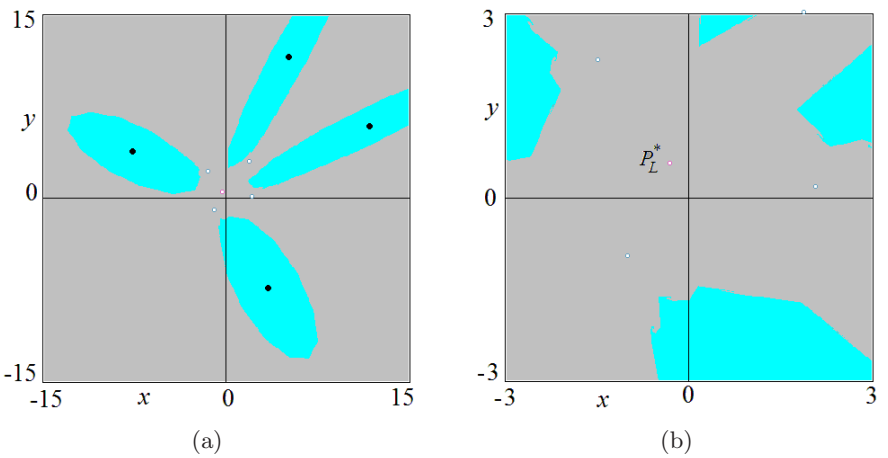

Fig. 12. In (a) $a = 1.11$, the basin of C_4^s is shown in azure, bounded by closed invariant curves, and gray points have divergent trajectories. In (b) enlargement, the shape of the boundary suggests a repelling closed curve made up by the connection of a saddle and a repelling focus cycle.

$\mathcal{B}(\mathcal{C}_4^s)$. The shape in the enlargement of Fig. 12(b) evidences a saddle-focus connection related to some cycle of high period, leading to the repelling closed invariant curve on the boundary.

After the center bifurcation almost all the trajectories are divergent, even if repelling cycles exist, besides P_L^*. Moreover, the pair of 4-cycles disappear at the fold-BCB at $a \simeq 1.334434$.

4. Bifurcations Related to the 3-Cycle

In the bifurcation sequences described in this section, we can see how several bifurcations of cases (A), (B) and (C) may occur. Moreover, the transition noninverible/invertible shows the route to many coexisting attracting cycles.

4.1. *Crossing over the upper center bifurcation curve*

For fixed value of a and increasing c (for $a > 0.5$ and $c > 1+\frac{a}{2}$) crossing the upper branch of the center bifurcation curve, a supercritical center bifurcation of the 3-cycle occurs, as shown in Sec. 2. Let us here describe the further bifurcation sequences occurring in the example for $a = 1$ and increasing c up to the disappearance of bounded attractors for map T. The supercritical center bifurcation leads to an attracting closed invariant curve which, due

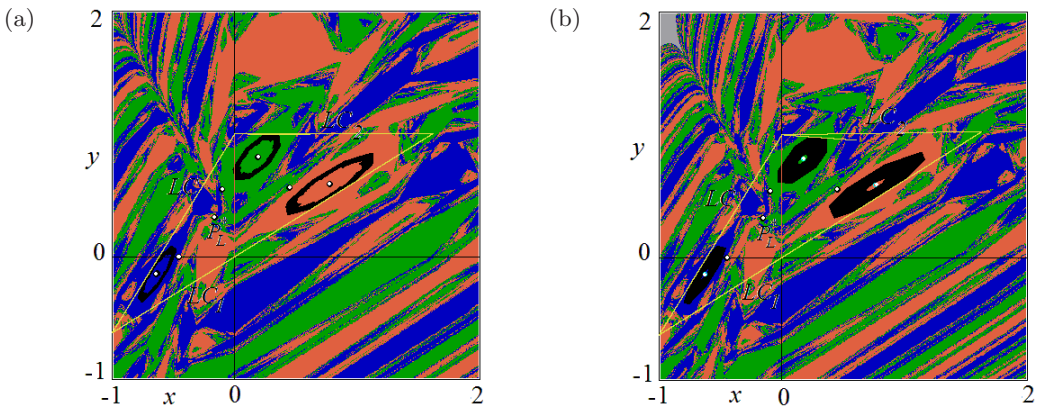

Fig. 13. Annular chaotic areas inside the invariant area. In (a) at $a = 1$, $c = 1.62$ annular chaotic area inside, and in (b) at $a = 1$, $c = 1.63$. The colors show evidence of the basins for map T^3.

to the noninvertibility of the map, develops into an annular chaotic area, as shown in Fig. 13. The internal and external boundaries of the invariant area consist of a finite number of images of the critical segment on LC_{-1} crossed by the area itself [Mira *et al.*, 1996].

As long as there is a hole around the repelling 3-cycle focus, the 3-cycle is not homoclinic. The first homoclinic bifurcation (snap-back repeller bifurcation of the 3-cycle focus, after [Marotto, 1978, 2005]) occurs when the critical lines cross through the points of the 3-cycle, after which the holes disappear [Gardini, 1994; Gardini *et al.*, 2011]. It is worth noticing that the three invariant areas belong to a wider absorbing area made up of three segments of critical curves, images of the segment $(0, 0) - (0, 1)$ on LC_{-1}. Let us denote $A_{-1} = (0, 0)$, as the starting point, then $A_0 = T(A_{-1}) = (0, 1)$ belongs to $LC_{-1} \cap LC$, where LC is given by $y = \frac{c}{a}x + 1$, a further image by the function $T_L(x, y)$ (i.e. for $LC \cap \{x \leq 0\}$) leads to $A_1 = T(A_0) = (-a, -(c - 1))$ which belongs to $LC \cap LC_1$, where a portion of LC_1 belongs to the straight line

$$LC_1 : \; y = \frac{c^2 - a}{a(1 + c)}x + \frac{1 - a}{1 + c} \tag{21}$$

which intersects LC_{-1} in $B_{-1} = (0, \frac{1-a}{1+c})$, and the image of the segment A_1B_{-1} is mapped by the function $T_L(x, y)$ into a segment of LC_2 belonging to the straight line

$$LC_2 : \; y = -\left(x + a\frac{1 - a}{1 + c}\right)\frac{a(1 + c) - c(c^2 - a)}{a(1 + c + c^2 - a)} + 1 - c\frac{1 - a}{1 + c} \tag{22}$$

connecting $A_2 = (ac, c^2 - c + 1 - a)$ to $B_0 = T(B_{-1}) = (\frac{a(a-1)}{1+c}, \frac{1+ac}{1+c})$.

In the case $a = 1$ we have that LC_1 (on $y = (c - 1)x$) crosses through $B_{-1} = (0, 0)$, $A_2 = (c, c^2 - c)$ and $B_0 = (0, 1) = A_0$ belongs to the portion of LC_2 on the line $y = x\frac{c^2-c-1}{c} + 1$, whose slope is positive for $c > \frac{1+\sqrt{5}}{2} \simeq 1.618$, and zero (leading to the line $y = 1$) for $c = \frac{1+\sqrt{5}}{2}$ which is the center bifurcation of the 3-cycle. It follows that at the center bifurcation of the 3-cycle the invariant triangle including the invariant polygons is given by the triangle connecting the points $A_0 = (0, 1)$, $A_1 = (-1, -c + 1)$ and $A_2 = (c, c^2 - c)$. After the center bifurcation, for $c > \frac{1+\sqrt{5}}{2}$, the triangle connecting the points $A_0 = (0, 1)$, $A_1 = (-1, -c + 1)$ and $A_2 = (c, c^2 - c)$ (which always includes $(0, 0)$) is invariant and includes all the attracting sets of map T.

After the snap-back repeller bifurcation of the 3-cycle focus, the three cyclic chaotic areas increase in size, as shown in Fig. 14(a), and a contact bifurcation with the basin boundary for map T^3 occurs for increasing c, also called expansion bifurcation [see Fig. 14(b)], leading to the reunion of the three areas into a unique invariant area $\mathcal{A}$ with chaotic dynamics which is the one connecting the points $A_0 = (0, 1)$, $A_1 = (-1, -c+1)$ and $A_2 = (c, c^2 - c)$. This area is the only attracting set, and the basin of attraction, separating bounded trajectories from divergent ones, that includes a repelling 2-cycle as well as its stable set (which consists of points as long as it is a repelling node, while includes segments when the 2-cycle is a saddle).

The appearance of a repelling 2-cycle occurs via degenerate transcritical bifurcation (case (C)), as

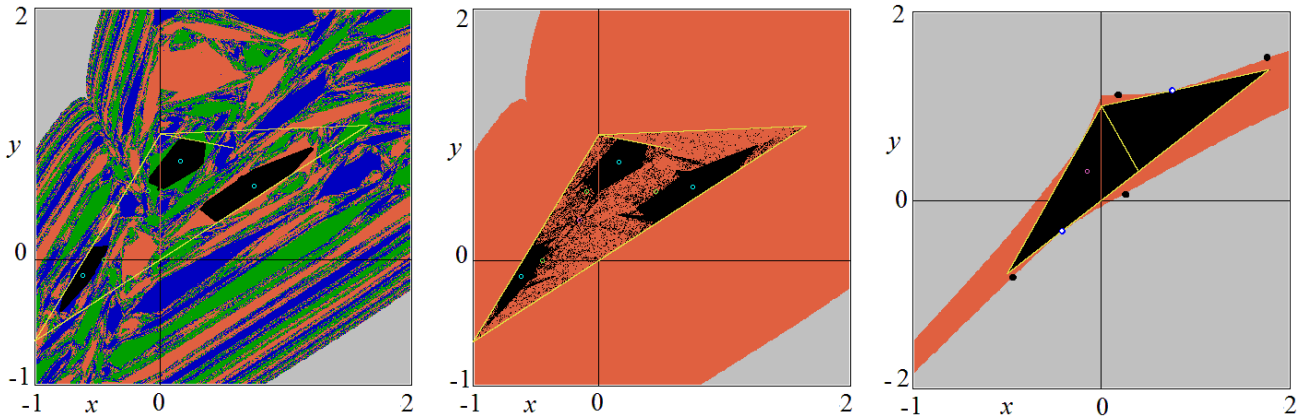

Fig. 14. In (a) at $a = 1$, $c = 1.648$, after the SBR bifurcation of the 3-cycle focus. In (b) at $a = 1$, $c = 1.6485$, after the contact bifurcation leading to a one-piece chaotic set. In (c) at $a = 1$, $c = 1.78$, close to the final bifurcation, leading to the disappearance of the attracting chaotic set. The points of the 2-cycle and 4-cycle on the frontier are evidenced.

already remarked in [Gardini & Tikjha, 2019]. In fact, looking for the solutions of the equation $T_L \circ T_R(x, y) = (x, y)$, considering

$$T_L \circ T_R(x,y) = \begin{bmatrix} -(1+a) & a(1+c) \\ (1-c) & (c^2-a) \end{bmatrix} \begin{bmatrix} x \\ y \end{bmatrix} + \begin{bmatrix} -a \\ 1-c \end{bmatrix} \tag{23}$$

we obtain a solution $\mathcal{C}_2^u = (x_{2,R}^u, y_{2,R}^u)$ given by

$$(x_{2,R}^u, y_{2,R}^u) = \left(\frac{a^2}{2c^2 - (a^2+2a+2)}, \frac{2(c-1)}{2c^2-(a^2+2a+2)} \right) \tag{24}$$

which belongs to the right partition for $x_{2,R}^u > 0$ which holds for $c > \sqrt{1 + a + \frac{a^2}{2}}$. In such a case, its image is

$$(x_{2,L}^u, y_{2,L}^u) = \left(\frac{a^2 - 2a(c-1)}{2c^2 - (a^2+2a+2)}, \frac{2(c-a-1)}{2c^2-(a^2+2a+2)} \right) \tag{25}$$

and $x_{2,L}^u < 0$ is always satisfied. From the Jacobian matrix, having trace $\mathrm{Tr}_{RL} = c^2 - 2a - 1$ and determinant $D_{RL} = -(c^2 - a^2)$, the characteristic polynomial $\mathcal{P}_{RL}(\lambda)$ leads to $\mathcal{P}_{RL}(1) = a^2 + 2a + 2 - 2c^2$, $\mathcal{P}_{RL}(-1) = a(a-2)$. Thus the single 2-cycle appears via degenerate transcritical bifurcation when $\mathcal{P}_{RL}(1) = 0$ [the denominator in (24) becomes zero] at

$$\tau(\mathcal{C}_2^u):\ c^2 = 1 + a + \frac{a^2}{2}. \tag{26}$$

For $c > \sqrt{1 + a + \frac{a^2}{2}}$ the 2-cycle $\mathcal{C}_2^u$ exists, and it is $\mathcal{P}_{RL}(1) < 0$ so that, of the two eigenvalues $\lambda_\pm = \frac{1}{2}((c^2 - 2a - 1) \pm \sqrt{(c^2-2a-1)^2 + 4(c^2-a^2)})$, it is always $\lambda_+ > 1$ (since increasing c, $\mathcal{P}_{RL}(1)$ decreases). Moreover, from $\mathcal{P}_{RL}(-1) = a(a-2)$ we have that for $a < 2$ the 2-cycle is a repelling node ($\lambda_- < -1$), while for $a > 2$ it is a saddle as long as $-1 < \lambda_- < 1$. The bifurcation value $a = 2$ will be commented on in the next subsection (it is a degenerate flip bifurcation of subcritical type).

So, for $a = 1$, the 2-cycle is a repelling node, with periodic points

$$\begin{aligned} (x_{2,R}^u, y_{2,R}^u) &= \left(\frac{1}{2c^2-5}, \frac{2(c-1)}{2c^2-5} \right), \\ (x_{2,L}^u, y_{2,L}^u) &= \left(\frac{3-2c}{2c^2-5}, \frac{2(c-2)}{2c^2-5} \right) \end{aligned} \tag{27}$$

belonging to the basin boundary. The final bifurcation, leading to almost all divergent trajectories, occurs when the invariant area $\mathcal{A}$ has a contact with the basin boundary. We can see that the final bifurcation takes place when the repelling 2-cycle merges with $\mathcal{A}$, which occurs when the periodic points merge with the critical curves, that is $(x_{2,L}^u, y_{2,L}^u) \in LC_1$ (or equivalently $(x_{2,R}^u, y_{2,R}^u) \in LC_2$). Considering the value of the parameter c such that

$$\frac{2(c-2)}{2c^2-5} = (c-1)\frac{3-2c}{2c^2-5} \tag{28}$$

we have $c = \frac{3+\sqrt{17}}{4} \simeq 1.780776$, as shown in Fig. 14(c).

However, the 2-cycle is not the only one belonging to the basin boundary. In fact, increasing c, for $c > a > 1$, also a repelling 4-cycle appears by degenerate transcritical bifurcation (one more case (C)), crossing a branch of the curve whose equation is given in (19), and a periodic point with symbolic sequence $RLRR$ is given in (15), but now it is not attracting, and it appears without a companion cycle $LLRR$. At the parameter values used in Fig. 14 this 4-cycle is a saddle, with eigenvalues $\lambda_1 > 1$ and $\lambda_2 \in (-1, 0)$.

This 2-cycle and this 4-cycle related to cases (C), will play a role also in the bifurcation sequences described in the next subsection.

4.2. *Crossing over the upper degenerate flip bifurcation curve*

The lower branch has been already commented on in Sec. 3.2, for $c = 0.2$ increasing the parameter a, and we have seen that it consists in a degenerate subcritical flip (an attracting 6-cycle merges with a repelling 3-cycle leading to an attracting 3-cycle).

Let us now fix a larger value of a such that increasing c, we cross the upper branch of the degenerate flip bifurcation curve. Let us first consider $a = 2$ fixed. Increasing the parameter c after the bifurcation value of the 3-cycle, an attracting set consisting of six chaotic pieces is observed, which increases quickly in size, becoming soon a one-piece chaotic set, bounded by the images of the critical segment of LC_{-1} which is included in the area. The frontier of the basin of attraction includes the 2-cycle and the 4-cycle saddles commented on above, which are in a particular configuration. In fact, for $a = 2$ we have $\mathcal{P}_{RL}(-1) = a(a-2) = 0$, which means that one eigenvalue is equal to -1, and so at the degenerate flip bifurcation, for any value of c. This means that the periodic point closest to $x = 0$ determines (on the eigenvector related to the eigenvalue -1) a segment filled with periodic points of period-4. In our case, this is the periodic point $(x^u_{2,L}, y^u_{2,L}) = \left(\frac{3-2c}{2c^2-5}, \frac{2(c-2)}{2c^2-5}\right)$ given in (25) and its stable set belongs to the frontier of the basin, see the blue segments in Fig. 15(a) leading to a 4-cycle on the boundary of the segments, which include a point on LC_{-1} ($x = 0$). This 4-cycle on the border corresponds to the 4-cycle mentioned above, which undergoes a border collision (it exists for $a < 2$, it does not exist for $a > 2$, showing one more example in which a unique cycle may appear/disappear, related to a degenerate flip bifurcation, case (B), of subcritical type, as we have seen also for the 3-cycle and 9-cycle in Sec. 3.2).

The periodic point of this 4-cycle having symbolic sequence $RRLR$ is the colliding one, fixed point of the function $T_R \circ T_L \circ T_R^2(x, y)$ given by

$$x_4 = \frac{a^2(a-2)(a-2c+2)}{a^4 - 2c^4 - 2a^3c + 2ac^3 + 4ac^2 - 2a^2 - 2ac + 2},$$
$$y_4 = \frac{-2(a^2 - a - ac^2 - c^2 + c^3 + c - 1)}{a^4 - 2c^4 - 2a^3c + 2ac^3 + 4ac^2 - 2a^2 - 2ac + 2} \quad (29)$$

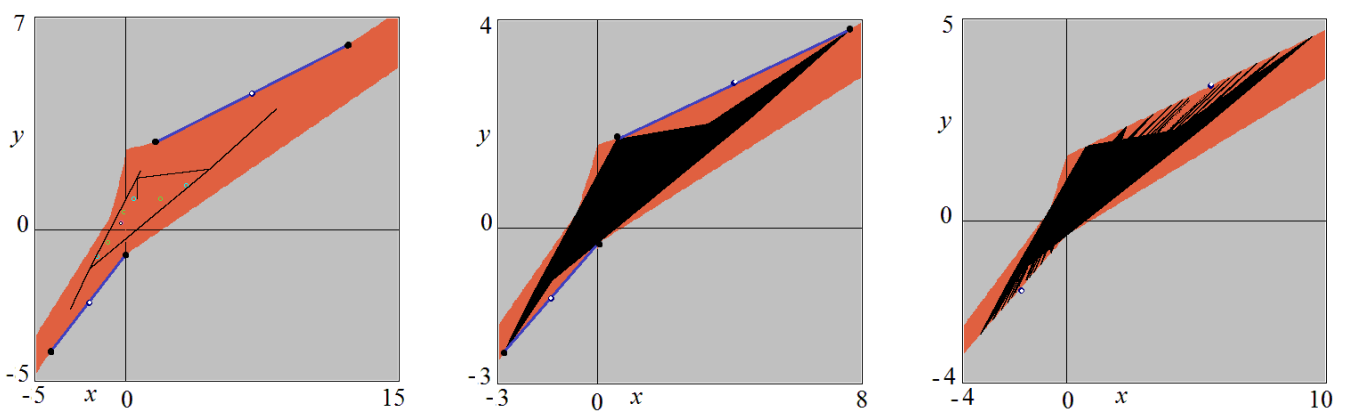

(a) (b) (c)

Fig. 15. In (a) at $a = 2$, $c = 2.3$, the 3-cycle is attracting. On the basin boundary, the blue segments are filled with 4-cycles of map T. In (b) at $a = 2$, $c = 2.342$, at the final bifurcation, leading to the disappearance of the attracting chaotic set, and BCB of the 4-cycle on the boundary of the two segments. In (c) at $a = 2.2$, $c = 2.461$, close to the final bifurcation, homoclinic bifurcation of the saddle 2-cycle, leading to the disappearance of the attracting chaotic set.

leading, for $a = 2$, to

$$x_4 = 0,$$
$$y_4 = \frac{-(c^3 - 3c^2 + c + 1)}{2c^3 + 4c^2 - c^4 - 10c + 5} = \frac{c^2 - 2c - 1}{(c-1)(c^2-5)} \quad (30)$$

and for any value of c it gives the border of the segments filled with 4-cycles of map T.

When the system consists of a unique chaotic piece, the final bifurcation as usual occurs, increasing c, when the chaotic area has a contact with its basin boundary. In our case, this occurs when the chaotic area has a contact with the 4-cycle, that is, when the periodic point $(x_4, y_4) \in LC_1$, which takes place when the following condition holds: $(x_4, y_4) = B_{-1}$, and it is satisfied when

$$\frac{c^2 - 2c - 1}{(c-1)(c^2-5)} = \frac{-1}{1+c} \quad (31)$$

that is, for c solution of

$$c^3 - c^2 - 4c + 2 = 0 \quad (32)$$

leading to $c \simeq 2.342923$ [the value used in Fig. 15(b) is very close to the bifurcation value].

As mentioned above, for $a > 2$ the 4-cycle no longer exists (disappeared via a border collision associated with a degenerate flip bifurcation), and on the frontier of the basin of attraction there is the 2-cycle saddle. In such cases, the final bifurcation (leading to almost all divergent trajectories) occurs at the homoclinic bifurcation of the 2-cycle saddle, an example is shown in Fig. 15(c).

4.3. *Transition noninvertible/invertible*

Let us now illustrate via the example at $c = 1$ fixed and increasing a, the transition which occurs in the phase space. Increasing a, the map is immediately noninvertible and chaotic (the real fixed point is never attracting), while for $a = 1$ the 3-cycle described in Sec. 2 is almost globally attracting and for $a > 1$ the map becomes invertible. Since increasing a from 0 the real fixed point is a repelling focus while the virtual fixed point is an attracting focus, the images of the critical curves rotate and lead to absorbing areas, which include all the attracting sets. An example is shown in Fig. 16(a), the images of the segment of LC_{-1} crossed by the invariant area give the boundaries. It is evident from the figure the existence of a 7-cycle repelling focus (inside the seven white holes), and as a increases its snap-back repeller bifurcation occurs, leading to an annular chaotic area, as in Fig. 16(b).

As a is further increased, the value $a = a^*$ at which the pair of 3-cycles appear by fold-BCB is approached ($a^* = \frac{3-\sqrt{5}}{2} \simeq 0.382$). We can characterize the bifurcation value of the fold-BCB also by using the critical lines. In fact, considering the images of the segment on LC_{-1} we obtain an absorbing area which includes the invariant chaotic area, in which a corner point is marked, and it belongs to the left side for $a < a^*$, to LC_{-1} for $a = a^*$ and to the right side for $a > a^*$ (see Fig. 17). At the bifurcation value, the point on LC_{-1} belongs to the 3-cycle, and it is at its fold-BCB [Fig. 17(b)]. For $a > a^*$ the wider area is invariant and includes all the attracting sets (the chaotic area and the

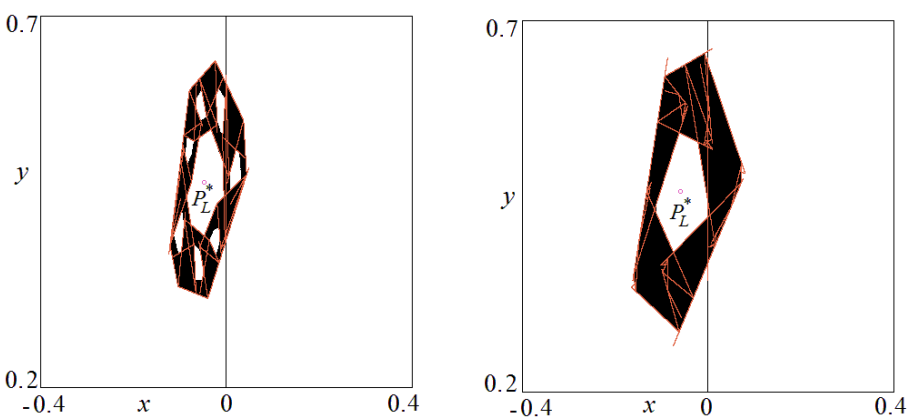

Fig. 16. Annular chaotic areas. In (a) at $c = 1$, $a = 0.2$. In (b) at $c = 1$, $a = 0.25$, after the SBR bifurcation of the 7-cycle repelling focus.

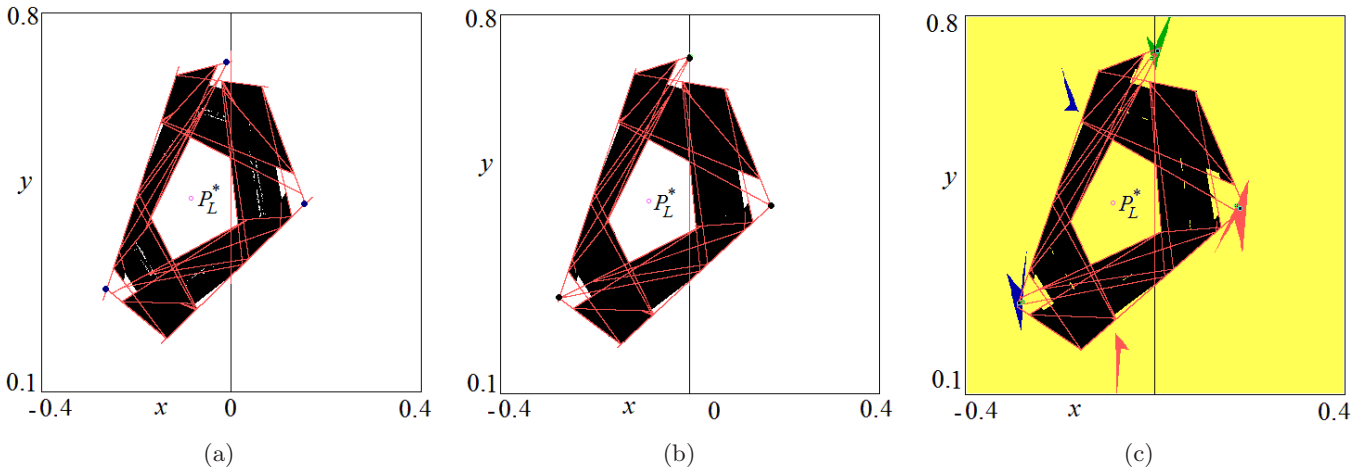

Fig. 17. Invariant areas bounded by segments of critical lines. In (a) at $c = 1$, $a = 0.37 < a^*$. In (b) at $c = 1$, $a = 0.3819$, close to a^*. In (c) at $c = 1$, $a = 0.395 > a^*$.

attracting 3-cycle). In Fig. 17(c) the basin of attraction of the chaotic area is in yellow, while three different colors emphasize the basins of the three attracting fixed points of map T^3 (clearly, only a few components are shown in that figure, since further preimages exist). Inside the wider area, increasing the parameter a the chaotic area approaches the stable set of the 3-cycle saddle, and the contact bifurcation will lead to its disappearance, that is, the invariant area no longer exists and we have the transition from a chaotic attractor to a chaotic repeller. This can be seen in Fig. 18(a), before the contact, the basin of the attracting 3-cycle is a disconnected set, bounded by the stable set of the 3-cycle saddle, which is not homoclinic (a few components of the basin are shown in Fig. 18(a) for map T^3), at the contact the homoclinic bifurcation of the saddle 3-cycle occurs, while soon after the contact bifurcation, the basins of the three fixed points of map T^3 have an explosion, with fractal basins' structure, and are still separated by the stable set of the 3-cycle saddle, now homoclinic, as shown in Fig. 18(b). It is worth noting that as long as the map is noninvertible (i.e. for $a < 1$) an absorbing area can be constructed, and we do not observe other attractors different from the 3-cycle. For $a > 1$ the map becomes invertible, and the basins of attraction of the fixed points of map T^3 become connected. Then, increasing the parameter a, other cycles may appear by BCB, coexisting with the attracting 3-cycle. The first one that we observe is shown in Fig. 19(a), where an attracting

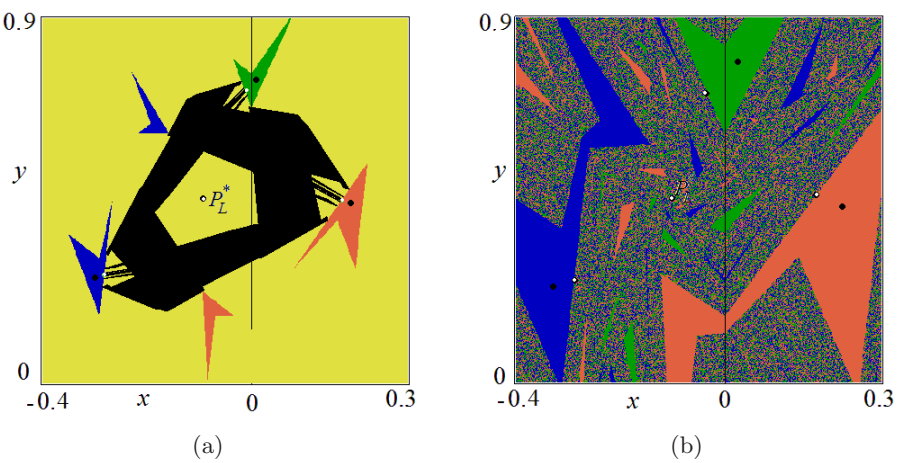

Fig. 18. In (a) at $c = 1$, $a = 0.4064$ close to the contact between the chaotic area and the stable set of the saddle 3-cycle, on the basin boundary of the attracting 3-cycle, homoclinic bifurcation of the saddle 3-cycle. In (b) at $c = 1$, $a = 0.45$ after the contact, the chaotic attractor no longer exists, while a chaotic repeller belongs to the boundaries of the basins of map T^3, having a fractal structure, and the 3-cycle saddle is homoclinic.

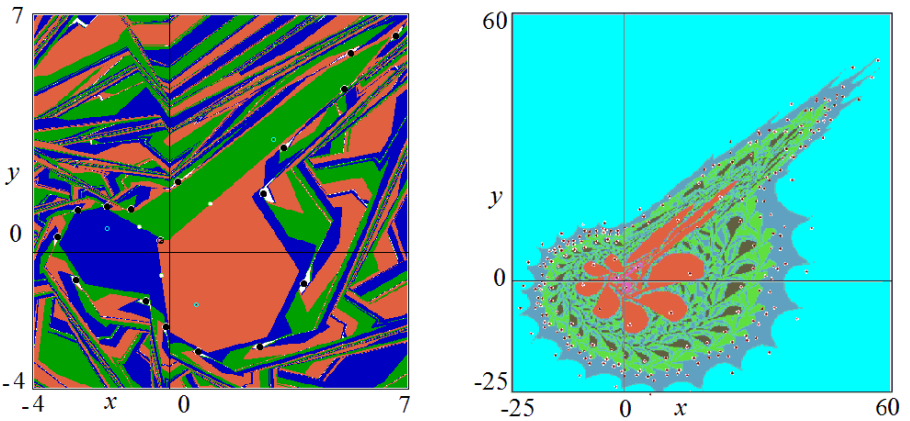

(a) (b)

Fig. 19. In (a) at $c = 1$, $a = 1.462$ the attracting 3-cycle coexists with an attracting cycle of period-16. In (b) at $c = 1$, $a = 1.516$ the attracting 3-cycle coexists with other five attracting cycles.

cycle of period-16 (appeared by fold-BCB) coexists with the 3-cycle. The basin of attraction of the 16-cycle is bounded by the stable set of a saddle cycle of period-16. Increasing a, more and more cycles appear via cases (A), coexisting with the 3-cycle. An example is shown in Fig. 19(b), where besides the 3-cycle, there exist also attracting cycles of periods-10, -27, -37, -64 and -92. Other cycles appear/disappear by BCB as a approaches the codimension-two point $a = \frac{1+\sqrt{5}}{2} \simeq 1.618$, intersection between the bifurcation curves $\det(J_{RLR}) = 1$ and SN-BCB$_{3,2}$, that is, intersection between the lower branch of the center bifurcation of the 3-cycle and the fold-BCB, leading to the disappearance of the 3-cycles.

5. Conclusions

In the present paper we have considered the different bifurcation mechanisms related to the appearance/disappearance of cycles in the two-dimensional piecewise continuous map T given in (2), describing their role in several bifurcation routes. The bifurcation mechanisms may be related to several cases, (A) fold border collision bifurcations, (B) degenerate flip bifurcations, (C) degenerate transcritical bifurcations and (D) supercritical center bifurcations, whose characteristics have been recalled in the Introduction. After the description of the existence and bifurcation regions of fixed points, 3-cycles and 4-cycles of map T given in Sec. 2, different bifurcation routes have been considered in Secs. 3 and 4. In Sec. 3, we have shown how bifurcations of cases (A) and (B) are involved with supercritical center bifurcations (case (D)) or center bifurcations of subcritical type. In particular, cases of degenerate flip bifurcations (cases (B)) of subcritical type have been evidenced, as well as the occurrence of a fold-BCB (case (A)) associated with two saddle cycles (which cannot occur in smooth maps). In Sec. 4, we have described several bifurcations related to an attracting 3-cycle, involving in particular degenerate transcritical bifurcations (cases (B)) associated with single repelling cycles, which belong to the frontier separating divergent trajectories. In that section we have also described the dynamics occurring in the transition from non-invertibility to invertibility of map T. The critical curves play a prominent role in the noninvertible cases, and are related to snap-back repeller bifurcations of several cycles, while in the invertible range sequences of many bifurcations of cases (A) lead to multistability.

Acknowledgments

The first author is supported by the Centre of Excellence in Mathematics, Thailand Research Fund and Pibulsongkram Rajabhat University, and is grateful to the University of Urbino for the hospitality during his visiting period. The work of L. Gardini has been done within the activities of the GNFM (National Group of Mathematical Physics, INDAM Italian Research Group).

References

Avrutin, V., Schanz, M. & Gardini, L. [2010] "On a special type of border-collision bifurcations occurring at infinity," *Physica D* **239**, 1083–1094.

Avrutin, V., Zhusubaliyev, Z. T., Saha, A., Banerjee, S., Sushko, I. & Gardini, L. [2016] "Dangerous bifurcations revisited," *Int. J. Bifurcation and Chaos* **26**, 1630040-1–24.

Banerjee, S. & Verghese, G. C. [2001] *Nonlinear Phenomena in Power Electronics*, *Attractors*, *Bifurcations*, *Chaos*, *and Nonlinear Control* (IEEE Press).

Bischi, G. I., Gardini, L. & Sushko, I. [2017] "Periodicity induced by production constraints in Cournot duopoly models with unimodal reaction curves," *Optimization and Dynamics with Their Applications*, ed. Matsumoto, A. (Springer).

Brogliato, B. [1999] *Nonsmooth Mechanics Models*, *Dynamics and Control* (Springer-Verlag, NY).

Burr, C., Gardini, L. & Szidarovszky, F. [2015] "Discrete time dynamic oligopolies with adjustment constraints," *J. Dyn. Games* **2**, 65–87.

di Bernardo, M., Budd, C. J., Champneys, A. R. & Kowalczyk, P. [2008] *Piecewise-Smooth Dynamical Systems*: *Theory and Applications*, Applied Mathematical Sciences, Vol. 163 (Springer).

Ganguli, A. & Banerjee, S. [2005] "Dangerous bifurcation at border collision: When does it occur?" *Phys. Rev. E* **71**, 057202-1–4.

Gardini, L. [1994] "Homoclinic bifurcations in n-dimensional endomorphisms, due to expanding periodic points," *Nonlin. Anal*: *Th. Meth. Appl.* **23**, 1039–1089.

Gardini, L., Sushko, I., Avrutin, V. & Schanz, M. [2011] "Critical homoclinic orbits lead to snap-back repellers," *Chaos Solit. Fract.* **44**, 433–449.

Gardini, L., Sushko, I. & Matsuyama, K. [2018] "2D discontinuous piecewise linear map: Emergence of fashion cycles," *Chaos* **28**, 055917.

Gardini, L. & Tikjha, W. [2019] "The role of virtual fixed points and center bifurcations in a piecewise linear map," *Int. J. Bifurcation and Chaos* **29**, 1930041-1–18.

Hassouneh, M. A., Abed, E. H. & Nusse, H. E. [2004] "Robust dangerous border-collision bifurcations in piecewise smooth systems," *Phys. Rev. Lett.* **92**, 070201.

Ma, Y., Agarwal, M. & Banerjee, S. [2006] "Border collision bifurcations in a soft impact system," *Phys. Lett. A* **354**, 281–287.

Marotto, F. [1978] "Snap-back repellers imply chaos in R^n," *J. Math. Anal. Appl.* **63**, 199–223.

Marotto, F. [2005] "On redefining a snap-back repeller," *Chaos Solit. Fract.* **25**, 25–28.

Mira, C., Gardini, L., Barugola, A. & Cathala, J. C. [1996] *Chaotic Dynamics in Two-Dimensional Noninvertible Maps* (World Scientific, Singapore).

Nusse, H. E. & Yorke, J. A. [1992] "Border-collision bifurcations including 'period two to period three' bifurcation for piecewise smooth systems," *Physica D* **57**, 39–57.

Nusse, H. E. & Yorke, J. A. [1995] "Border-collision bifurcations for piecewise smooth one dimensional maps," *Int. J. Bifurcation and Chaos* **5**, 189–207.

Radi, D., Gardini, L. & Avrutin, V. [2014] "The role of constraints in a segregation model: The symmetric case," *Chaos Solit. Fract.* **66**, 103–119.

Radi, D. & Gardini, L. [2015] "Entry limitations and heterogeneous tolerances in a Schelling-like segregation model," *Chaos Solit. Fract.* **79**, 130–144.

Radi, D. & Gardini, L. [2018] "A piecewise smooth model of evolutionary game for residential mobility and segregation," *Chaos* **28**, 055912.

Simpson, D. J. W. & Meiss, J. D. [2008] "Neimark–Sacker bifurcations in planar, piecewise-smooth, continuous maps," *SIAM J. Appl. Dyn. Syst.* **7**, 795–824.

Simpson, D. J. W. [2010] *Bifurcations in Piecewise-Smooth Continuous Systems* (World Scientific).

Simpson, D. J. W. [2014a] "Sequences of periodic solutions and infinitely many coexisting attractors in the border-collision normal form," *Int. J. Bifurcation and Chaos* **24**, 1430018-1–18.

Simpson, D. J. W. [2014b] "Scaling laws for large numbers of coexisting attracting periodic solutions in the border-collision normal form," *Int. J. Bifurcation and Chaos* **24**, 1450118-1–28.

Sushko, I. & Gardini, L. [2008] "Center bifurcation for two-dimensional border-collision normal form," *Int. J. Bifurcation and Chaos* **18**, 1029–1050.

Sushko, I. & Gardini, L. [2010] "Degenerate bifurcations and border collisions in piecewise smooth 1D and 2D maps," *Int. J. Bifurcation and Chaos* **20**, 2045–2070.

Sushko, I., Avrutin, V. & Gardini, L. [2015] "Bifurcation structure in the skew tent map and its application as a border collision normal form," *J. Diff. Eqs. Appl.* **22**, 1040–1087.

Tikjha, W., Lapierre, E. G. & Sitthiwirattham, T. [2017] "The stable equilibrium of a system of piecewise linear difference equations," *Adv. Diff. Eqs.* **67**, 1–10.

Zhusubaliyev, Zh. T. & Mosekilde, E. [2003] *Bifurcations and Chaos in Piecewise-Smooth Dynamical Systems*, World Scientific Series on Nonlinear Science A, Vol. 44 (World Scientific).